Physics Letters B 781 (2018) 206–212

Contents lists available at ScienceDirect

Physics Letters B

www.elsevier.com/locate/physletb

A resolution of the inclusive flavor-breaking τ $|V_{us}|$ puzzle

Renwick J. Hudspith [a], Randy Lewis [a], Kim Maltman [b,*,1], James Zanotti [c]

[a] Department of Physics and Astronomy, York University, 4700 Keele St., Toronto, ON, M3J 1P3, Canada
[b] Department of Mathematics and Statistics, York University, 4700 Keele St., Toronto, ON, M3J 1P3, Canada
[c] CSSM, Department of Physics, University of Adelaide, Adelaide, SA 5005, Australia

ARTICLE INFO

Article history:
Received 10 February 2017
Received in revised form 19 February 2018
Accepted 28 March 2018
Available online 3 April 2018
Editor: B. Grinstein

ABSTRACT

We revisit the puzzle of $|V_{us}|$ values obtained from the conventional implementation of hadronic-τ-decay-based flavor-breaking finite-energy sum rules lying $> 3\sigma$ below the expectations of three-family unitarity. Significant unphysical dependences of $|V_{us}|$ on the choice of weight, w, and upper limit, s_0, of the experimental spectral integrals entering the analysis are confirmed, and a breakdown of assumptions made in estimating higher dimension, $D > 4$, OPE contributions identified as the main source of these problems. A combination of continuum and lattice results is shown to suggest a new implementation of the flavor-breaking sum rule approach in which not only $|V_{us}|$, but also $D > 4$ effective condensates, are fit to data. Lattice results are also used to clarify how to reliably treat the slowly converging $D = 2$ OPE series. The new sum rule implementation is shown to cure the problems of the unphysical w- and s_0-dependence of $|V_{us}|$ and to produce results ~ 0.0020 higher than those of the conventional implementation employing the same data. With B-factory input, and using, in addition, dispersively constrained results for the $K\pi$ branching fractions, we find $|V_{us}| = 0.2231(27)_{exp}(4)_{th}$, in excellent agreement with the result from $K_{\ell 3}$, and compatible within errors with the expectations of three-family unitarity, thus resolving the long-standing inclusive τ $|V_{us}|$ puzzle.

1. Introduction

With $|V_{ud}| = 0.97417(21)$ [1] as input and $|V_{ub}|$ negligible, 3-family unitary implies $|V_{us}| = 0.2258(9)$. Direct determinations of $|V_{us}|$ from $K_{\ell 3}$ and $\Gamma[K_{\mu 2}]/\Gamma[\pi_{\mu 2}]$, using recent 2014 FlaviaNet experimental results [2] and 2016 lattice input [3] for $f_+(0)$ and f_K/f_π, respectively, yield results, $|V_{us}| = 0.2231(9)$ and 0.2253(7), in agreement with this expectation. In contrast, the most recent update [4] of the conventional implementation of the finite-energy sum rule (FESR) determination employing flavor-breaking (FB) combinations of inclusive strange and non-strange hadronic τ decay data [5], yields $|V_{us}| = 0.2186(21)$, 3.1σ below 3-family-unitarity expectations. A less discrepant, but still low, result, 0.2207(27), was obtained in Ref. [6] using the same conventional implementation but somewhat higher input $K\pi$ branching fractions (resulting from an analysis of $K\pi$ data imposing additional dispersive constraints on the timelike $K\pi$ form factors [6]). The general FB FESR framework whose conventional implementation produces these low $|V_{us}|$ results is outlined below.

In the Standard Model, the differential distributions, $dR_{V/A;ij}/ds$, for flavor $ij = ud, us$, vector (V) or axial-vector (A) current-mediated decays, with $R_{V/A;ij}$ defined by $R_{V/A;ij} \equiv \Gamma[\tau^- \to \nu_\tau \text{ hadrons}_{V/A;ij}(\gamma)]/\Gamma[\tau^- \to \nu_\tau e^- \bar{\nu}_e(\gamma)]$, are related to the spectral functions, $\rho^{(J)}_{V/A;ij}$, of the $J = 0, 1$ scalar polarizations, $\Pi^{(J)}_{V/A;ij}$, of the corresponding current–current two-point functions, by [7]

$$\frac{dR_{V/A;ij}}{ds} = \frac{12\pi^2 |V_{ij}|^2 S_{EW}}{m_\tau^2}\left[w_\tau(y_\tau)\rho^{(0+1)}_{V/A;ij}(s) - w_L(y_\tau)\rho^{(0)}_{V/A;ij}(s)\right] \equiv \frac{12\pi^2 |V_{ij}|^2 S_{EW}}{m_\tau^2}(1-y_\tau)^2\,\tilde{\rho}_{V/A;ij}(s)\,, \quad (1)$$

where $y_\tau = s/m_\tau^2$, $w_\tau(y) = (1-y)^2(1+2y)$, $w_L(y) = 2y(1-y)^2$, S_{EW} is a known short-distance electroweak correction [8], and V_{ij} is the flavor ij CKM matrix element. The $J = 0$ spectral functions, $\rho^{(0)}_{A;ud,us}(s)$, are dominated by the accurately known, chirally unsuppressed π and K pole contributions. The remaining, continuum

* Corresponding author.
E-mail addresses: renwick.james.hudspith@gmail.com (R.J. Hudspith), randy.lewis@yorku.ca (R. Lewis), kmaltman@yorku.ca (K. Maltman), james.zanotti@adelaide.edu.au (J. Zanotti).
[1] Alternate address: CSSM, Department of Physics, University of Adelaide, Adelaide, SA 5005, Australia.

https://doi.org/10.1016/j.physletb.2018.03.074

contributions to $\rho^{(0)}_{V/A;ud,us}(s)$ are $\propto (m_i \mp m_j)^2$, and hence negligible for $ij = ud$. For $ij = us$, they are small (though not totally negligible) and highly constrained, through the associated $ij = us$ scalar and pseudoscalar sum rules, by the known value of m_s, making possible mildly model-dependent determinations in the range $s \le m_\tau^2$ relevant to hadronic τ decays [9,10]. Subtracting the resulting $J = 0$ contributions from the RHS of Eq. (1) yields the $J = 0+1$ analogue, $dR^{(0+1)}_{V/A;ij}/ds$, of $dR_{V/A;ij}/ds$, from which the $J = 0+1$ spectral function combinations $\rho^{(0+1)}_{V/A;ud,us}(s)$ can be determined.

The inclusive τ determination of $|V_{us}|$ employs FB FESRs for the spectral function combination, $\Delta\rho(s) \equiv \rho^{(0+1)}_{V+A;ud}(s) - \rho^{(0+1)}_{V+A;us}(s)$ and associated polarization difference, $\Delta\Pi(Q^2) \equiv \Pi^{(0+1)}_{V+A;ud}(Q^2) - \Pi^{(0+1)(Q^2)}_{V+A;us}$ [5], with $Q^2 = -s$. Generically, for any $s_0 > 0$ and any choice of analytic weight $w(s)$,

$$\int_0^{s_0} w(s)\Delta\rho(s)\,ds = -\frac{1}{2\pi i}\oint_{|s|=s_0} w(s)\Delta\Pi(-s)\,ds\,. \tag{2}$$

For large enough s_0, the OPE is used on the RHS.

Defining the re-weighted integrals

$$R^w_{V+A;ij}(s_0) \equiv \int_0^{s_0} ds\,\frac{w(s)}{w_\tau(s)}\,\frac{dR^{(0+1)}_{V+A;ij}(s)}{ds}\,, \tag{3}$$

and using Eq. (2) to replace the FB difference

$$\delta R^w_{V+A}(s_0) \equiv \frac{R^w_{V+A;ud}(s_0)}{|V_{ud}|^2} - \frac{R^w_{V+A;us}(s_0)}{|V_{us}|^2}\,, \tag{4}$$

with its OPE representation, one finds, solving for $|V_{us}|$ [5],

$$|V_{us}| = \sqrt{R^w_{V+A;us}(s_0)\Big/\left[\frac{R^w_{V+A;ud}(s_0)}{|V_{ud}|^2} - \delta R^{w,OPE}_{V+A}(s_0)\right]}\,. \tag{5}$$

The result is necessarily independent of s_0 and w so long as all input is reliable. Assumptions employed in evaluating $\delta R^{w,OPE}_{V+A}(s_0)$ can thus be tested for self-consistency by varying w and s_0. OPE assumptions entering the conventional implementation of the FB FESR approach in fact produce $|V_{us}|$ displaying significant w- and s_0-dependence [11].

The low $|V_{us}|$ results noted above are produced by a conventional implementation of the general FB FESR framework, Eq. (5), in which a single s_0 ($s_0 = m_\tau^2$) and single weight ($w = w_\tau$), are employed [5]. This restriction allows the $ij = ud$ and us spectral integrals to be determined from the inclusive ud and us branching fractions alone, but precludes carrying out s_0- and w-independence tests. Since w_τ has degree 3, $\delta R^{w_\tau,OPE}_{V+A}(s_0)$ receives contributions up to dimension $D = 8$. While $D = 2$ and 4 contributions, determined by α_s and the quark masses and condensates [3,12–15], are known, $D > 4$ contributions are not. In the conventional implementation, $D = 6$ contributions are estimated using the vacuum saturation approximation (VSA) (see Ref. [16] for the explicit expression) and $D = 8$ contributions neglected [5,11]. These assumptions are potentially dangerous since the FB V+A VSA estimate involves a very strong double cancellation,[2] and the VSA is known to be badly violated, in a channel-dependent manner, from studies in the non-strange sector [17].

[2] A factor of ~ 3 reduction occurs when the individual ud and us V+A sums are formed, and a further factor of ~ 6 reduction in forming the FB $ud - us$ V+A difference.

Such assumptions can, in principle, be tested by varying s_0. Writing $D > 4$ contributions to $\Delta\Pi(Q^2)$ as $\sum_{D>4} C_D/Q^D$, with C_D the effective dimension D condensate, the integrated $D = 2k+2$ OPE contribution to the RHS of Eq. (2), for a polynomial weight $w(y) = \sum_{n=0} w_n y^n$ with $y = s/s_0$, is, up to α_s-suppressed logarithmic corrections,

$$-\frac{1}{2\pi i}\oint_{|s|=s_0} ds\,w(y)\left[\Delta\Pi(Q^2)\right]^{OPE}_{D=2k+2} = (-1)^k\,w_k\,\frac{C_{2k+2}}{s_0^k}\,. \tag{6}$$

Problems with the assumptions employed for C_6 and C_8 in the conventional implementation will thus manifest themselves as an unphysical s_0-dependence in the $|V_{us}|$ results obtained using weights $w(y)$ with non-zero coefficients, w_2 and/or w_3, of y^2 and y^3.

Another potential issue for the FB FESR approach is the slow convergence of the $D = 2$ OPE series. To four loops, neglecting $O(m^2_{u,d}/m^2_s)$ corrections [12]

$$\left[\Delta\Pi(Q^2)\right]^{OPE}_{D=2} = \frac{3}{2\pi^2}\,\frac{\bar m_s}{Q^2}\left[1 + \frac{7}{3}\bar a + 19.93\bar a^2 + 208.75\bar a^3\right], \tag{7}$$

where $\bar a = \alpha_s(Q^2)/\pi$, and $\bar m_s = m_s(Q^2)$, $\alpha_s(Q^2)$ are the running strange mass and coupling in the $\overline{MS}$ scheme. With $\bar a(m_\tau^2) \simeq 0.1$, the ratio of $O(\bar a^3)$ to $O(\bar a^2)$ terms is > 1 at the spacelike point on $|s| = s_0$ for all kinematically accessible s_0. Such slow "convergence" complicates choosing an appropriate truncation order and estimating the associated truncation uncertainty.

No apparent convergence problem exists for the $D = 4$ series, which, to three loops, dropping numerically tiny $O(m_q^4)$ terms, is given by [13]

$$\left[\Delta\Pi(Q^2)\right]^{OPE}_{D=4} = \frac{2\left[\langle m_u\bar uu\rangle - \langle m_s\bar ss\rangle\right]}{Q^4}\left(1 - \bar a - \frac{13}{3}\bar a^2\right). \tag{8}$$

The slow convergence of the $D = 2$ OPE series and the reliability of conventional implementation assumptions for C_6 and C_8 will be investigated in the next section.

In the rest of the paper, the non-strange and strange spectral distributions entering the various FESRs considered are fixed using $\pi_{\mu 2}$, $K_{\mu 2}$ and SM expectations for the π and K pole contributions, recent ALEPH data for the continuum ud V+A distribution [18], Belle [19] and BaBar [20] results for the $K^-\pi^0$ and $\bar K^0\pi^-$ distributions, BaBar results [21] for the $K^-\pi^+\pi^-$ distribution, Belle results [22] for the $\bar K^0\pi^-\pi^0$ distribution, a combination of BaBar [24] and Belle [25] results for the very small $\bar KKK$ distribution, and 1999 ALEPH results [23] for the combined "residual mode" distribution (the sum over contributions from those strange modes not remeasured by the B-factory experiments). BaBar and Belle exclusive strange mode distributions are given in unit-normalized form, with measured branching fractions required to set the overall scales. We work, in general, with 2016 HFAG [26] branching fractions. For the two $K\pi$ modes, however, we consider also the alternate results, $B[\tau \to K^-\pi^0\nu_\tau] = 0.004707(181)$ and $B[\tau \to \bar K^0\pi^-\nu_\tau] = 0.008566(299)$, obtained in Ref. [6] (ACLP), from an analysis imposing additional dispersive constraints on the timelike $K\pi$ form factors. The corresponding 2016 HFAG $K\pi$ results, obtained without the dispersive constraints, are $B[\tau \to K^-\pi^0\nu_\tau] = 0.004327(149)$ and $B[\tau \to \bar K^0\pi^-\nu_\tau] = 0.008386(141)$.

A plot of the latest version of the ALEPH ud V+A spectral distribution may be found in Ref. [18]. The exclusive- and residual-mode contributions to the continuum us V+A distribution, in the form, $|V_{us}|^2\,\tilde\rho_{V+A;us}(s)$, directly determinable from the experiment, are shown in Fig. 1. For definiteness, the $K\pi$ points are shown with

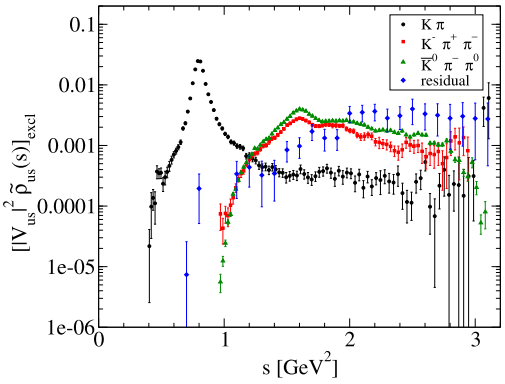

Fig. 1. Exclusive- and residual-mode contributions to the continuum $|V_{us}|^2\,\tilde{\rho}_{V+A;us}(s)$ distribution, with 2016 HFAG normalization for the $K\pi$ points.

the 2016 HFAG $K\pi$ normalization. A global rescaling of 1.044 is required to convert these to the alternate 2013 ACLP $K\pi$ normalization.

We base our central results on the additionally-constrained ACLP input choice, but quote results obtained using both $K\pi$ normalizations. Note that the publicly available ALEPH continuum *ud* V+A distribution is normalized to a slightly older version of the inclusive *ud* continuum branching fraction. A small rescaling (0.5% or less) is required to convert this to the normalization implied by the branching fractions we employ. The normalizations of the different components of the 1999 ALEPH residual mode distribution are also updated using HFAG 2016 branching fractions [26].

2. Testing conventional implementation assumptions

The conventional implementation assumptions, $C_6 \simeq C_6^{VSA}$ and $C_8 = 0$, can be efficiently investigated using appropriately chosen s_0- and w-independence tests. A comparison of the results of the $w_\tau(y) = 1 - 3y^2 + 2y^3$ and $\hat{w}(y) = 1 - 3y + 3y^2 - y^3$ FESRs is particularly illuminating since the coefficients of y^2 in the two weights differ only by a sign. The corresponding integrated $D = 6$ OPE contributions are thus identical in magnitude but opposite in sign. If, as the VSA estimate suggests, $D = 6$ contributions are small for w_τ, they must also be small for $\hat{w}$. Similarly, if integrated $D = 8$ contributions are negligible for w_τ, those for $\hat{w}$, which are $-1/2$ times as large, will also be negligible. If conventional implementation assumptions for C_6 and C_8 are reliable, the $|V_{us}|$ obtained from the w_τ and $\hat{w}$ FESRs should thus be in good agreement, and show good individual s_0 stability. In contrast, if these assumptions are not reliable, and $D = 6$ and $D = 8$ contributions are not both small, one should see s_0-instabilities of opposite signs in the two cases, and s_0-dependent differences in the results from the two FESRs which decrease with increasing s_0.

The central values of the results of this comparison, obtained using the ACLP and HFAG $K\pi$ normalizations, and, to be specific, the 3-loop-truncated contour-improved (CIPT) prescription [27] for handling the integrated $D = 2$ OPE series, are shown in the top left and bottom left panels of Fig. 2, respectively, and clearly, in both cases, correspond to the second scenario. One should bear in mind that the results for a given weight but different s_0 are strongly correlated, as are the w_τ and $\hat{w}$ results at the same s_0. Neither changing the $D = 2$ truncation order nor switching from CIPT to the alternate fixed-order (FOPT) $D = 2$ prescription for the $D = 2$ series serves to remove the strong, unphysical s_0 and weight dependences.

To understand the extent to which the s_0- and w-instabilities shown in Fig. 2 are a problem for the conventional implementation $D > 4$ condensate assumptions, it is useful to consider the differences between the $|V_{us}|$ obtained from the $\hat{w}$ and w_τ FESRs at the same s_0. If the conventional implementation assumptions are reliable these differences should be zero within errors. Fully propagating the *ud* and *us* experimental covariances, and adding independent sources of theory error in quadrature, we find, however, $\hat{w}$-w_τ differences of $0.0234\,(5)_{exp}\,(38)_{th}$ at $s_0 = 1.95$ GeV^2, $0.0111\,(8)_{exp}\,(21)_{th}$ at $s_0 = 2.55$ GeV^2, and $0.0064\,(16)_{exp}\,(13)_{th}$ at $s_0 = 3.15$ GeV^2, clearly signalling problems with the conventional implementation assumptions. Similar conclusions follow from the observed s_0-instabilities. For example, the difference between the $\hat{w}$ FESR results at $s_0 = 2.55$ GeV^2 and 3.15 GeV^2, which should once more be zero within errors, is instead $0.0039\,(5)_{exp}\,(8)_{th}$. A similarly discrepant result, $0.0096\,(8)_{exp}\,(19)_{th}$, is found for the difference between the $s_0 = 2.15$ GeV^2 and 3.15 GeV^2 $\hat{w}$ results.

The top right and bottom right panels of Fig. 2 show the results of corresponding additional w- and s_0-independence tests involving the weights $w_N(y)$, $N = 2, 3, 4$, with[3]

$$w_N(y) = 1 - \frac{N}{N-1}y + \frac{1}{N-1}y^N\,. \tag{9}$$

The upper solid lines in each case show the w_2, w_3 and w_4 results obtained using the conventional implementation treatment of $D > 4$ OPE contributions and given $K\pi$ normalization, while the dashed–dotted show lines the corresponding results produced by the alternate implementation discussed below, in which the $D > 4$ effective condensates are fit to experimental data. The corresponding conventional and alternate implementation w_τ results (represented by the lowest solid and dotted lines, respectively) are also included for comparison. The latter are obtained using the $D = 6$ and 8 effective condensates obtained from the alternate implementation w_2 and w_3 fits. The s_0-dependent, conventional implementation results for all of w_τ, $\hat{w}$, w_2, w_3 and w_4 show evidence of converging toward a common value at $s_0 > m_\tau^2$, as expected if the observed s_0-instabilities result from $D > 4$ OPE contributions larger than those taken as input in the conventional implementation.

The impact of the slow convergence of the $D = 2$ OPE series can be investigated by comparing OPE expectations to lattice results for $\Delta\Pi(Q^2)$ over a range of Euclidean $Q^2 = -q^2 = -s$, using variously truncated versions of the $D = 2$ OPE series. Lattice results were obtained using the RBC/UKQCD $n_f = 2 + 1$, $32^3 \times 64$, $1/a = 2.38$ GeV, domain wall fermion ensemble with $m_\pi \sim 300$ MeV [29]. A tight cylinder cut, with a radius determined in a recent study of the extraction of α_s from lattice current–current two-point function data [30], was imposed to suppress lattice artifacts at higher Q^2. The values of the light quark masses, $m_u = m_d \equiv m_\ell$ and m_s, for this ensemble, determined in Ref. [29], were used for determining the corresponding OPE expectations.

We consider the comparison first for larger Q^2, where $D = 2$ and 4 contributions should dominate. The $D = 2$ OPE contribution is determined using ensemble values of m_u and m_s [29], the central PDG value for α_s [14], and considering 2-, 3- and 4-loop truncation of the $D = 2$ series. Both fixed scale, $\mu^2 = 4$ GeV^2, and local scale, $\mu^2 = Q^2$, choices for handling the logarithms in the truncated series are considered. The former choice is the analogue of the fixed order (FOPT) prescription for the $D = 2$ FESR contour integrals, the latter the analogue of the alternate CIPT prescription.[4] For $D = 4$ contributions, Eq. (8), we employ the Gell-Mann–Oakes–Renner (GMOR) relation for $\langle m_u \bar{u}u\rangle$ and fix $\langle m_s \bar{s}s\rangle$

[3] The $w_N(y)$, like $w_\tau(y)$, have a double zero at $s = s_0$ ($y = 1$). This serves to keep duality violating contributions safely small above $s \simeq 2$ GeV^2 [28].

[4] The FOPT prescription evaluates weighted $D = 2$ OPE integrals using a fixed-scale choice (usually $\mu^2 = s_0$), the CIPT prescription [27] using the local-scale choice, $\mu^2 = Q^2$.

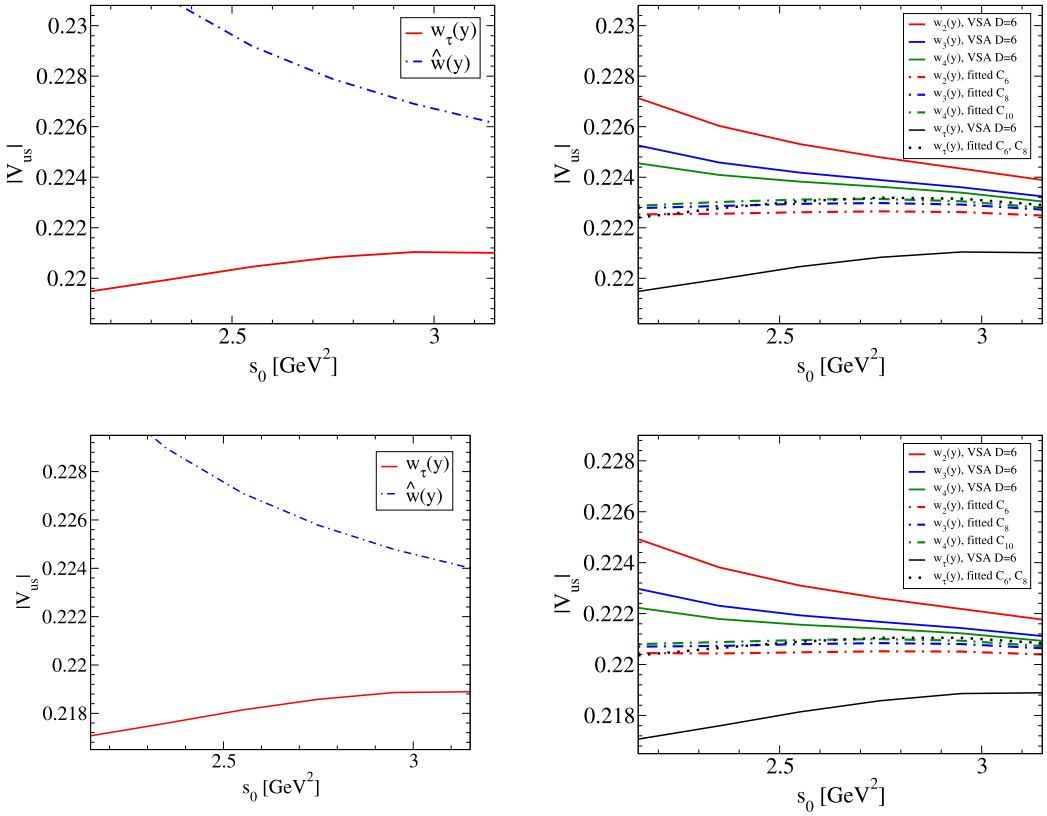

Fig. 2. Left panels: conventional implementation w_τ (bottom curve) and $\hat{w}$ (top curve) results for $|V_{us}|$. Right panels: w_N and w_τ FESR results obtained using the fixed-order (FOPT) $D=2$ prescription. Solid lines show, top to bottom, conventional implementation results for w_2, w_3, w_4 and w_τ. Dashed–dotted lines show, bottom to top, w_2, w_3 and w_4 results, and the dotted line w_τ results, obtained using central $C_{6,8}$ fit values from the alternative FB FESR analyses described in the text. Figures in the first row show results obtained using the ACLP $K\pi$ normalization, those in the second row those obtained using the HFAG $K\pi$ normalization.

using the ensemble value of m_s/m_ℓ, translating the HPQCD result for $\langle\bar{s}s\rangle/\langle\bar{\ell}\ell\rangle$ at physical quark masses [15], to that for the ensemble masses using NLO ChPT [31].

The comparisons obtained using the fixed- and local-scale versions of the $D=2$ series are shown in the left and right panels of Fig. 3, respectively. The best representation of the lattice results is provided by the 3-loop-truncated, fixed-scale version, which produces an excellent match over a wide range of Q^2, extending from near ~ 10 GeV^2 down to just above ~ 4 GeV^2, with the Q^2 dependence of the lattice results also favoring the fixed-scale over the alternate local-scale treatment.[5]

Comparison to the lattice results also provides two further useful pieces of information. The left panel of Fig. 4 shows the comparison of the lattice results, the three-loop-truncated, fixed-scale $D=2$ series version of the $D=2+4$ OPE sum, and this same $D=2+4$ OPE sum now supplemented by the VSA estimate for $D=6$ contributions, in the lower Q^2 region. Below ~ 4 GeV^2, the lattice results clearly require $D>4$ OPE contributions much larger than those assumed in the conventional implementation, confirming the conclusions reached already from the w_τ-$\hat{w}$ FESR comparison above. The right panel shows the comparison of the lattice results and three-loop-truncated, fixed-scale $D=2$ series $D=2+4$ OPE sum, now with the conventionally estimated errors for the latter also displayed. These are obtained by combining in quadrature standard estimates for the $D=4$ truncation errors with uncertainties produced by those on the input $D=2$ and 4 OPE parameters. Despite the apparently problematic convergence behavior of the $D=2$ series, conventional OPE error estimates are seen to provide an extremely conservative assessment of the uncertainty for the $D=2+4$ sum.

3. An alternate implementation of the FB FESR approach

The results of the previous section suggest an obvious alternative to the conventional implementation of the FB FESR approach. First, the 3-loop-truncated FOPT treatment favored by the comparison to the high-Q^2 lattice results is employed for the $D=2$ OPE integrals.[6] Second, since both lattice and continuum results suggest that conventional implementation assumptions for the effective $D>4$ condensates, C_D, are unreliable, we avoid such assumptions and instead fit the C_D to data. FESRs based on the weights $w_N(y)$ are particularly convenient for use in fitting the $C_{D>4}$ since the w_N-weighted OPE integral involves only a single $D>4$ contribution, $(-1)^N C_{2N+2}/\left[(N-1)\,s_0^N\right]$. The s_0 dependence of the w_N-weighted spectral integrals in the region above

[5] Note that both the lattice data and OPE results at different Q^2 are highly correlated. These correlations (and not just the errors on the individual OPE and lattice points) must be taken into account to assess the significance (or lack thereof) of the difference in the Q^2 dependences of the local-scale OPE and lattice results. The uncertainty on the Q^2 dependence is, in fact, strongly dominated by that on the input strange-to-light condensate ratio. Taking all correlations into account, one finds, for the fixed- and local-scale versions of the ratio of OPE to lattice values of the average slope between, for example, $Q^2\simeq 5$ GeV^2 and $Q^2\simeq 9$ GeV^2, the results 1.02(14) and 1.20(17), respectively, with (13) and (16) of the quoted errors coming from the uncertainty on the input strange-to-light condensate ratio. The Q^2 dependence of the lattice data thus favors the fixed-scale treatment of the $D=2$ series.

[6] It is worth noting that the prescription of truncating at 3-loop order is also what one would arrive at were one to interpret the series as asymptotic and truncate it at its smallest term.

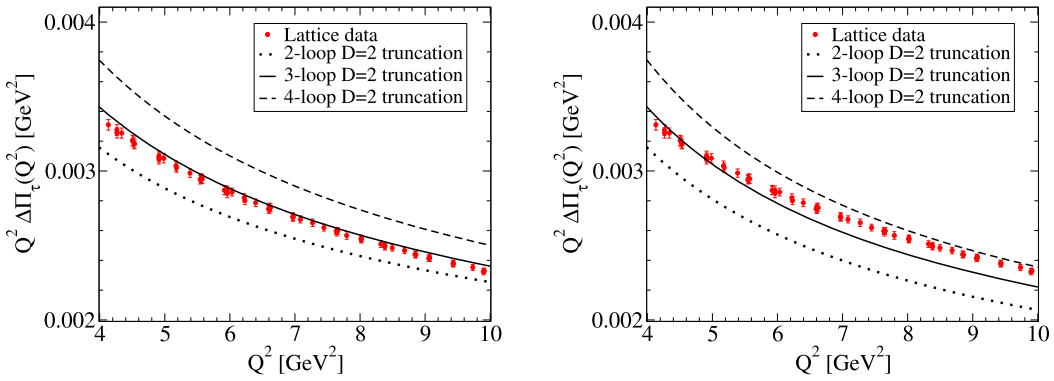

Fig. 3. Comparison of lattice results and $D=2+4$ OPE expectations for $Q^2\,\Delta\Pi_\tau(Q^2)$, for either fixed-scale (left panel) or local-scale (right panel) treatments of the $D=2$ series.

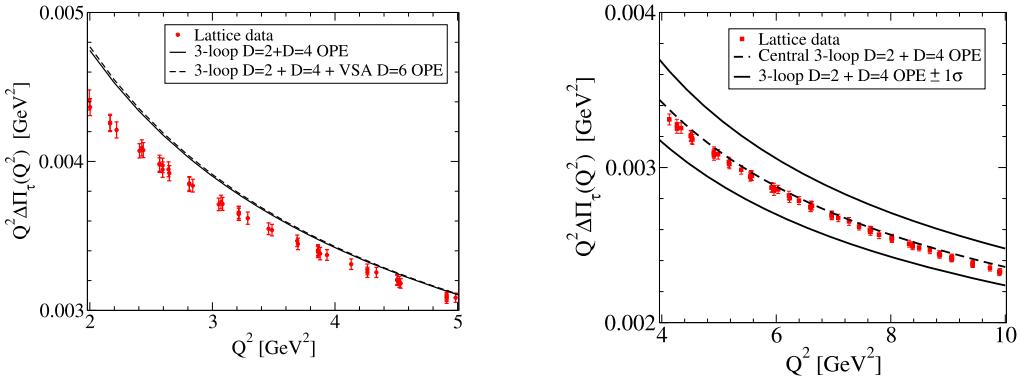

Fig. 4. Left panel: Comparison of lower-Q^2 lattice results to $D=2+4$ and $D=2+4+6$ OPE expectations (fixed-scale, 3-loop truncation for $D=2$, VSA for $D=6$). Right panel: Lattice results and the $D=2+4$ OPE sum at larger Q^2, with conventional OPE error estimates (fixed-scale, 3-loop-truncated $D=2$).

$s_0 \sim 2$ GeV^2, where residual duality violations remain small, then provides sufficient information to allow both unknowns, $|V_{us}|$ and C_{2N+2}, entering the w_N FESR to be determined.

Spectral distribution inputs employed in our analysis were outlined above.[7] On the OPE side, for the $D=2$ and 4 contributions, we use PDG input for α_s [14], FLAG input for the light and strange quark masses [3], GMOR for the light-quark condensate [33], and the HPQCD lattice result [15] for the ratio of strange to light quark condensates. The single-weight w_2, w_3 and w_4 FESR $|V_{us}|$ fit results obtained using our central (ACLP) choice of $K\pi$ normalization, $0.2228\,(27)_{exp}\,(4)_{th}$, $0.2230\,(27)_{exp}\,(4)_{th}$ and $0.2232\,(27)_{exp}\,(4)_{th}$, respectively, show a dramatically reduced weight dependence relative to those of the obtained using conventional implementation assumptions for the $D>4$ condensates. This is also true of the analogous results, $0.2205\,(23)_{exp}\,(4)_{th}$, $0.2208\,(23)_{exp}\,(4)_{th}$ and $0.2209\,(23)_{exp}\,(4)_{th}$, obtained using the alternate HFAG $K\pi$ normalization. It is worth commenting that, although the lattice results for Euclidean Q^2 favor the fixed-scale treatment of the $D=2$ series, and hence, by extension, the FOPT prescription for the weighted $D=2$ FESR integrals, the final results for $|V_{us}|$ are rather insensitive to choosing FOPT over CIPT. Explicitly, the alternate CIPT choice yields $0.2229\,(27)_{exp}\,(4)_{th}$ for all of the w_2, w_3 and w_4 FESRs when the ACLP $K\pi$ normalization is used and $0.2206\,(23)_{exp}\,(4)_{th}$ when the HFAG $K\pi$ normalization is used. The CIPT treatment, of course, generates slightly different fit results for the $C_{D>4}$, as expected, given that FOPT and CIPT represent different partial resummations of the presumably asymptotic $D=2$ series.

[7] Note also that, when using the ACLP $K\pi$ normalization, we have, for consistency, implemented the long-distance electromagnetic corrections employed in arriving at the $K\pi$ branching fraction results obtained from the ACLP analysis [32].

Table 1
Single-weight fit $|V_{us}|$ error contributions for the w_2, w_3 and w_4 FESRs, using 3-loop-truncated FOPT for the $D=2$ OPE series. Notation as described in the text.

Source	$\delta\|V_{us}\|$ / w_2 FESR	$\delta\|V_{us}\|$ / w_3 FESR	$\delta\|V_{us}\|$ / w_4 FESR
$\delta\alpha_s$	0.00002	0.00006	0.00006
$\delta m_s(2\text{ GeV})$	0.00008	0.00009	0.00008
$\delta\langle m_s\bar{s}s\rangle$	0.00035	0.00035	0.00035
$\delta(J=0\ sub)$	0.00009	0.00009	0.00009
δ_{ud}^{exp}	0.00027	0.00028	0.00028
δ_{us}^{exp}	0.00272	0.00273	0.00273

Given the excellent consistency of the individual w_2, w_3 and w_4 FESR determinations, we take our final result from a combined 3-weight fit. The central ACLP $K\pi$ normalization choice yields

$$|V_{us}| = 0.2231\,(27)_{exp}\,(4)_{th}\,, \tag{10}$$

0.0022 higher than the result obtained using conventional implementation $D>4$ assumptions with the same experimental input. This result is in excellent agreement with the result from $K_{\ell 3}$ and compatible within errors with the expectations of 3-family unitarity. The combined 3-weight fit result, $|V_{us}| = 0.2208\,(23)_{exp}\,(4)_{th}$, generated by the alternate (HFAG) choice of $K\pi$ normalization, similarly, lies 0.0020 above the result obtained employing the same experimental input and conventional implementation assumptions for the $D>4$ condensates.

Table 1 shows the error budgets for the w_2, w_3 and w_4 fits employing the ACLP $K\pi$ normalization. Theory errors, resulting

from uncertainties in the input parameters α_s, m_s and $\langle m_s\bar{s}s\rangle$, and the small $J=0$ continuum subtraction, are labelled by $\delta\alpha_s$, δm_s, $\delta\langle m_s\bar{s}s\rangle$ and $\delta(J=0\ sub)$, respectively, and shown above the horizontal line. Those induced by the covariances of the non-strange and strange experimental distributions $dR_{V+A;ud}/ds$ and $dR_{V+A;us}/ds$ are denoted δ_{ud}^{exp} and δ_{us}^{exp} and shown below the horizontal line. The δ_{us}^{exp} uncertainties strongly dominate the total errors. From the lattice-OPE comparison discussed above, the estimates in the upper half of the table should provide a very conservative assessment of theoretical uncertainties. Combining the different components in quadrature yields a total theory error of 0.0004 on $|V_{us}|$ for all three determinations. The new implementation of the FB FESR approach is thus competitive with the alternate $K_{\ell 3}$ and $\Gamma[K_{\mu 2}]/\Gamma[\pi_{\mu 2}]$ determinations from a theory error point of view, though improvements to the errors on the strange experimental distributions are required to make it fully competitive over all.

To test whether fitting the $D>4$ condensates has solved the problem of the s_0-instabilities found in the conventional implementation, we have rerun the s_0-dependent w_N analyses, using the central fitted C_{2N+2} values as input.[8] The dashed–dotted lines in the right panel of Fig. 2 show the results of this exercise. Using the fitted $C_{D>4}$ values dramatically reduces the s_0-instabilities of the conventional implementation versions of the same analyses, providing a strong self-consistency check on the new FB FESR implementation. The dotted line in this same panel shows the analogous $|V_{us}|$ results obtained from the s_0-dependent w_τ analysis using the fitted values of C_6 and C_8 as input. One again finds a dramatic reduction in the s_0 dependence, as well as excellent agreement with the results obtained using the other weights.

Errors on the us distribution data limit the precision with which the C_{2N+2} (which represent nuisance parameters for the determination of $|V_{us}|$) can be currently determined. It is, nonetheless, worth checking that the results for the FB condensates are compatible with an expected FB suppression relative to the corresponding flavor ud V+A condensates. Comparing the results for C_6 and C_8 from our favored (FOPT) fits to those for the corresponding ud V+A condensates, $C_{6,8}^{ud;V+A}$, obtained from the favored, $s_{min}=1.55$ GeV^2, 3-weight, combined V&A FOPT fit of Ref. [17], we find, for the ratios of FB to non-FB $D=6$ and 8 condensates, the results 0.50(16)(20) and 0.40(25)(19), respectively, where the first error, in each case, results from the uncertainty on the FB condensate C_{2N+2} and the second from that on $C_{2N+2}^{ud;V+A}$. The results for the FB condensates are thus natural, and compatible with the expectation of FB suppression; the sizeable uncertainties, however, preclude going beyond these qualitative observations.

4. Conclusions

We have revisited the determination of $|V_{us}|$ from flavor-breaking finite-energy sum rule analyses of experimental inclusive non-strange and strange hadronic τ decay distributions, identifying an important systematic problem in the conventional implementation of this approach, and developing an alternate implementation which cures this problem. We have also used lattice results to bring under better theoretical control the treatment of the potentially problematic $D=2$ OPE series entering these analyses. The new implementation, which employs the FOPT prescription for the integrated $D=2$ OPE series and requires fitting effective $D>4$ condensates to data, dramatically reduces the w- and s_0-instabilities found when conventional implementation assumptions are employed for the $D=6,8$ condensates. The w- and s_0-instabilities of the conventional implementation establish that the assumptions employed in that implementation are not self-consistent, and hence that the conventional implementation needs to be abandoned going forward.

It is worth commenting on the relation to earlier attempts to bring the unphysical w- and s_0-dependence of the results for $|V_{us}|$ under improved control. Refs. [34,35] employed degree 8, 10 and 20 weights constructed to simultaneously (i) emphasize $D=2$ contributions from the part of the contour with lower $|\alpha_s(Q^2)|$, with the goal of improving the convergence of the $D=2$ series integrated using the CIPT prescription, and (ii) keep the coefficients w_N, $N\geq 2$ in $w(y)=\sum_N w_N y^N$, which govern $D>4$ OPE contributions, relatively small [36]. Relative to the weights $w_N(y)$ employed above, the earlier weights have the disadvantage of producing large numbers of experimentally unconstrained $D>4$ contributions, several governed by coefficients larger than those appearing in the $w_N(y)$. Focusing on the "ACO" section of Table II of Ref. [34], which employs strange exclusive branching fractions closest to (if slightly higher than) those used here, we find, not surprisingly, s_0-dependences significantly larger than those found from the new implementation employing the lower degree w_N, which choices allow the relevant $D>4$ effective condensates to be fit to data, rather than neglected as in cases of the weights used in Refs. [34,35]. Similarly, the weight-dependence of the $s_0=m_\tau^2$ $|V_{us}|$ results quoted in Ref. [35] is significantly larger than that found from the new implementation, quoted above. The new implementation thus also supercedes those earlier attempts to address the same w- and s_0-dependence problems.

The new implementation produces results for $|V_{us}|\sim 0.0020$ higher than those obtained analyzing the same data using conventional implementation assumptions for the $D=6$ and 8 condensates. Taking into account the additional dispersive constraints incorporated by the ACLP $K\pi$ normalization, we find a result, Eq. (10), in excellent agreement with that obtained from $K_{\ell 3}$, and compatible within errors with the expectations of three-family unitarity, thus resolving the long-standing puzzle of the $>3\sigma$ low values of $|V_{us}|$ obtained from the conventional implementation of the FB FESR τ approach.

Roughly half of the increase from the 0.2186(21) conventional implementation result for $|V_{us}|$ quoted in Ref. [4] comes from the shift to the ACLP $K\pi$ normalization and half from the use of the new implementation strategy. The use of results for the $D>4$ condensates obtained from fits to data in place of the non-self-consistent conventional implementation assumptions for these condensates is a particularly important feature of the new implementation.

The FB FESR approach to the determination of $|V_{us}|$ has been shown to have very favorable theory errors. The limitations, at present, are entirely experimental in nature, with errors strongly dominated by those on the weighted inclusive strange spectral integrals. In this regard, it is worth noting that the errors on the lower-multiplicity *exclusive-mode* $K^-\pi^0$, $\bar{K}^0\pi^-$, $K^-\pi^+\pi^-$ and $\bar{K}^0\pi^-\pi^0$ contributions, all of which are based on the much higher statistics BaBar and Belle distribution data are, at present, dominated by the uncertainties on the corresponding branching fractions (which normalize the unit-normalized experimental distributions). Significant improvements to the overall error can thus be achieved through improvements to the strange exclusive-mode branching fractions without requiring simultaneous, experimentally more difficult, improvements to the associated differential distributions.

[8] It is worth noting that the central fitted $C_{2N+2>4}$ produce contributions to the w_N FESRs which appear natural in size relative to the known $D=2$ and 4 contributions. At $s_0=m_\tau^2$, for example, relative to the corresponding $D=2$ contributions, $D=4$ and 6 contributions are $\sim 83\%$ and -26% for w_2, $D=4$ and 8 contributions $\sim 67\%$ and -11% for w_3, and $D=4$ and 10 contributions $\sim 61\%$ and -5% for w_4.

Acknowledgements

Thanks to RBC/UKQCD for providing access to the data of Ref. [29], used in the OPE-lattice study of the conventional FB FESR implementation. Lattice propagator inversions were performed on the STFC-funded "DiRAC" BG/Q system in the Advanced Computing Facility at the University of Edinburgh. The work of R.J.H., R.L. and K.M. is supported by the Natural Sciences and Engineering Research Council of Canada, that of J.M.Z. by Australian Research Council grants FT100100005 and DP140103067.

References

[1] J.C. Hardy, I.S. Towner, Phys. Rev. C 91 (2015) 015501.
[2] See, e.g., M. Moulson, arXiv:1411.5252 [hep-ex].
[3] S. Aoki, et al., Eur. Phys. J. C 77 (2017) 112.
[4] See the HFLAV-Tau Spring 2017 report, www.slac.stanford.edu/xorg/hfag/tau/spring-2017.
[5] E. Gamiz, et al., J. High Energy Phys. 0301 (2003) 060;
E. Gamiz, et al., Phys. Rev. Lett. 94 (2005) 011803;
E. Gamiz, et al., PoS KAON 2007 (2008) 008.
[6] M. Antonelli, V. Cirigliano, A. Lusiani, E. Passemar, J. High Energy Phys. 1310 (2013) 070.
[7] Y.-S. Tsai, Phys. Rev. D 4 (1971) 2821.
[8] J. Erler, Rev. Mex. Fis. 50 (2004) 200.
[9] M. Jamin, J.A. Oller, A. Pich, Nucl. Phys. B 587 (2000) 331;
M. Jamin, J.A. Oller, A. Pich, Nucl. Phys. B 622 (2002) 279;
M. Jamin, J.A. Oller, A. Pich, Phys. Rev. D 74 (2006) 074009. Thanks to Matthias Jamin for providing the results of the most recent of these analyses.
[10] K. Maltman, J. Kambor, Phys. Rev. D 65 (2002) 074013.
[11] K. Maltman, et al., Nucl. Phys. B, Proc. Suppl. 189 (2009) 175;
K. Maltman, Nucl. Phys. B, Proc. Suppl. 218 (2011) 146.
[12] P.A. Baikov, K.G. Chetyrkin, J.H. Kuhn, Phys. Rev. Lett. 95 (2005) 012003.
[13] K.G. Chetyrkin, A. Kwiatkowski, Z. Phys. C 59 (1993) 525, arXiv:hep-ph/9805232.
[14] C. Patrignani, et al., Particle Data Group, Chin. Phys. C 40 (2016) 100001.
[15] C. McNeile, et al., Phys. Rev. D 87 (2013) 034503.
[16] A. Pich, J. Prades, J. High Energy Phys. 9910 (1999) 004.
[17] D. Boito, et al., Phys. Rev. D 85 (2012) 093015;
D. Boito, et al., Phys. Rev. D 91 (2015) 034003.
[18] M. Davier, A. Hoecker, B. Malaescu, C.Z. Yuan, Z. Zhang, Eur. Phys. J. C 74 (2014) 2803.
[19] D. Epifanov, et al., Belle Collaboration, Phys. Lett. B 654 (2007) 65. For the $K_s\pi^-$ invariant mass spectrum see belle.kek.jp/belle/preprint/2007-28/tau_kspinu.dat. Thanks to Denis Epifanov for providing access to this data.
[20] B. Aubert, et al., BaBar Collaboration, Phys. Rev. D 76 (2007) 051104.
[21] I.M. Nugent, et al., BaBar Collaboration, Nucl. Phys. B, Proc. Suppl. 253–255 (2014) 38. Thanks to Ian Nugent for the providing the unfolded $K^-\pi^-\pi^+$ distribution and covariances.
[22] S. Ryu, et al., Belle Collaboration, Nucl. Phys. B, Proc. Suppl. 253–255 (2014) 33;
S. Ryu, et al., Belle Collaboration, Phys. Rev. D 89 (2014) 072009.
[23] R. Barate, et al., ALEPH Collaboration, Eur. Phys. J. C 11 (1999) 599. Thanks to Shaomin Chen for providing access to the mode-by-mode distributions and covariances.
[24] B. Aubert, et al., BaBar Collaboration, Phys. Rev. Lett. 100 (2008) 011801.
[25] M.J. Lee, et al., Belle Collaboration, Phys. Rev. D 81 (2010) 113007.
[26] Y. Amhis, et al., HFAG, arXiv:1612.07233.
[27] A.A. Pivovarov, Z. Phys. C 53 (1992) 461, Sov. J. Nucl. Phys. 54 (1991) 676, Yad. Fiz. 54 (1991) 1114;
F. Le Diberder, A. Pich, Phys. Lett. B 289 (1992) 165.
[28] K. Maltman, Phys. Lett. B 440 (1998) 367;
C.A. Dominguez, K. Schilcher, Phys. Lett. B 448 (1999) 93;
K. Maltman, T. Yavin, Phys. Rev. D 78 (2008) 094020.
[29] Y. Aoki, et al., RBC Collaboration, UKQCD Collaboration, Phys. Rev. D 83 (2011) 074508.
[30] R.J. Hudspith, R. Lewis, K. Maltman, E. Shintani, PoS LATTICE2015 (2016) 268.
[31] J. Gasser, H. Leutwyler, Nucl. Phys. B 250 (1985) 465.
[32] We thank the authors of Ref. [6] for providing their long-distance electromagnetic correction results, in numerical form.
[33] M. Gell-Mann, R.J. Oakes, B. Renner, Phys. Rev. 175 (1968) 2195.
[34] K. Maltman, C.E. Wolfe, Phys. Lett. B 639 (2006) 283.
[35] K. Maltman, C.E. Wolfe, Phys. Lett. B 650 (2007) 27.
[36] J. Kambor, K. Maltman, Phys. Rev. D 62 (2000) 093023.